

RS-LDPC Concatenated Coding for the Modern Tape Storage Channel

Jieun Oh, Jeongseok Ha, *Member, IEEE*, Hyegyeong Park, *Student Member, IEEE*,
and Jaekyun Moon, *Fellow, IEEE*

Abstract—In modern tape storage, user data are recorded and retrieved along multiple tracks of rapidly moving, flexible magnetic medium that give rise to a variety of channel impediments including occasional long erasures, more frequent amplitude fades as well as a large amount of random errors. This work considers reliable recovery of data from such tape channels using a novel concatenation of an inner Reed-Solomon (RS) code and an outer nonbinary low-density parity-check (LDPC) code. This particular concatenation scheme and a highly tailored iterative decoding algorithm are chosen to efficiently handle the assortment of the tape channel impediments while meeting the stringent target error rate constraint as well as key practical requirements of the mass tape storage system. Despite the use of a nonbinary LDPC code, the proposed scheme allows excellent performance-complexity tradeoffs. In stark contrast to any existing coding schemes that involve LDPC codes, the proposed concatenation strategy allows semianalytic error rate performance evaluation at rates below what is possible using modern computers, thus providing an ability to ensure satisfactory low-error-rate performance.

Index Terms—Channel coding, error correction codes, tape recording.

I. INTRODUCTION AND MOTIVATION

THE ADVENT of social networking coupled with the emergence of the Internet of Things fuels exponential growth in user data, which leads to huge demands on data storage. Among various types of mass storage devices, tape storage continues to be a viable choice for backing-up and archiving massive amounts of data [1] due to its notable advantages in capacity, cost, endurance and power consumption. While tape storage has continuously evolved in the direction of providing higher and higher bit densities over the past few decades, the ever-increasing demand for storage capacity calls for an accelerated effort in the same direction. Such efforts, unfortunately, always face serious challenges in maintaining the data integrity. In particular, the bit density improvement in modern tape systems has been mainly driven by increase in track

Manuscript received May 20, 2015; revised October 7, 2015; accepted November 19, 2015. Date of publication November 30, 2015; date of current version January 14, 2016. This work has been supported in part by the Tape Program in Information Storage Industry Consortium, the National Research Foundation of Korea (NRF) Grants (No. 2010-0029205 and No. 2015R1A2A2A01007739) funded by the Korea Government (MISP), and the BK21 Plus. The associate editor coordinating the review of this paper and approving it for publication was D. Declercq.

The authors are with the Department of Electrical Engineering Korea Advanced Institute of Science and Technology, Daejeon 305-701, South Korea (e-mail:jieunoh@kaist.ac.kr; sk8ergirlv@kaist.ac.kr; jsha@kaist.edu; jmooon@kaist.edu).

Digital Object Identifier 10.1109/TCOMM.2015.2504362

density, which has resulted in an inevitable deterioration of data reliability [2]–[4].

Data reliability in storage systems is usually guaranteed by employing error-control codes which should be carefully designed to handle error characteristics specific to the target storage channel. The tape storage channel is marred by a combination of impediments including broad-band noise, short fades, and long erasure dropouts due to a variety of material and mechanical imperfections such as media noise, thermal asperities, head-medium space variations, media defects and synchronization losses [5], [6]. In what is called the linear tape-open (LTO) standard [5]–[8], an error-control system with a RS-based two-dimensional product code and hard-decision decoding is employed for handling tape-specific errors. The RS product code, called RS-RS concatenation hereafter, is known to provide a very strong error-correcting capability in the presence of the characteristic long dropouts while offering fairly robust protection against random errors at a reasonable complexity level. Moreover, the RS-RS scheme is designed to support an important tape-specific requirement, namely, *read-after-write verification* for enabling tape systems to read and validate data immediately after they are written. This prevents the system from storing data on highly unreliable, defect areas of the tape.

While error-control using the above-mentioned RS-RS concatenation is widely deployed in current tape systems, as the track density gets higher, the signal-to-noise ratio (SNR) decreases proportionally to a point where the RS-RS concatenation is no longer able to protect data. Thus, a stronger error-control system well-tailored to tape medium is critical for developing next-generation tape storage. To this end, there have been some notable research works [9]–[14], where LDPC codes were considered for improved error control. In [9], performance of LDPC codes was investigated on real data taken off high-density metal particle media. The study in [9] concluded that LDPC codes were appropriate for tape recording systems in which the per-channel data rate requirement is significantly lower than that of hard disk drives. Meanwhile, in [10], [11], the outer RS code in the RS-RS concatenation were replaced with a packet LDPC code. In these works, the inner RS decoder converts a tape channel into an erasure channel by marking the symbols of failed codewords as erasures. While packet LDPC codes with the erasure filling decoder provide outstanding performance, the scheme does not always take full advantage of received signals from the tape channel since the symbols in the failed inner RS codewords are treated as erasures.

The noisy channel of the future tape media will be in a much lower SNR regime than that of today's tape drives [1]. Thus, it would make sense to develop error control systems that utilize soft information from the channel while also possessing strong burst error correction capability. In addition, the read-after-write verification feature must be supported.

To meet the above requirements, we consider an error-control system in which the outer RS code in the existing RS-RS concatenation code is replaced with a non-binary LDPC code and an iterative decoding scheme between the inner and outer codes is employed. The proposed coding scheme will be called RS-LDPC concatenation in the sequel. It should be noted that while algebraic codes are often chosen as outer codes [15], [16], in the proposed RS-LDPC concatenation, we deliberately choose RS codes as the inner code for the following reasons: 1) the inner RS code makes implementation of read-after-write verification straightforward via on-the-fly decoding of the inner code and 2) decoding complexity for a non-binary LDPC code can be significantly reduced when the outer decoder takes the hard decisions of the inner RS decoder as inputs. Meanwhile, the outer LDPC codes over higher-order Galois fields may be able to provide a large coding gain even for moderate codeword lengths [17], [18] as well as providing a more natural fit for the given inner-outer code concatenation since the inner code is non-binary as well.

In the proposed error-control system, the inner RS decoder conducts traditional hard-decision decoding. The outer LDPC decoder either takes the hard symbol decisions out of the RS decoder as clean symbols or, when the RS decoder fails, uses soft information from the channel. The LDPC decoder outputs are fed back to the RS decoder which retries decoding on the codewords that failed in the first place. The decoding for the outer LDPC codes is subsequently done. The process continues in this fashion until either the LDPC decoder generates valid codewords for the entire user data or enough attempts have been made. In the iterative decoding, the complexity of soft-decoding for the non-binary LDPC codes becomes manageable as the inner RS decoder makes clean hard decisions most of the times, which has an effect of removing the majority of the edges in the factor graph representation of the LDPC code. The combination of RS-LDPC concatenation and soft-decision decoding for the outer LDPC codes is already studied in [19] in an effort to combat the effect of impulsive noise in power-line-communications channel. However, the work in [19] adopts binary LDPC codes as outer codes.

The present work is different from the previous works [10], [11], [19] in that our decoder improves performance over iterations between inner and outer codes, whereas none of [10], [11], [19] employs inner-outer iteration. The selective use of either hard decisions out of the inner RS decoder or the soft channel equalizer outputs as the inputs of the outer decoder is also a unique feature of our work. The utilization of hard RS decoder outputs during the vast majority of time is what allows the practical deployment of the usually very-complex non-binary LDPC code, which is in contrast with the works of [10], [11], [19], all based on binary LDPC codes. In addition, for the packet-LDPC codes in [10], [11], performance evaluations are carried out only in limited cases. On the contrary, we evaluate

performances of the proposed error-control scheme under various channel conditions - intersymbol interference, long and short dropouts/fades, random errors - representing realistic tape storage systems. More importantly, in the previous works [10], [11], [19], performance evaluations are carried out with computer simulations. However, the target error-rates of storage systems are set too low to be evaluated with computer simulations. As is well known, for any coding scheme involving LDPC codes, performance evaluation in the low-error rate regime, where *trapping sets* limit the performance potential, is an open problem [20]. While many researchers have attempted to solve the error floor problem caused by the trapping sets by modifying LDPC encoders [21]–[27] or by proposing decoder-based strategies [28]–[30], the challenge of lowering error floors without increasing the encoder/decoder complexity or decoding latency remains high. Accordingly, the performance of the coding methods proposed in [10], [11], [19] could not be validated in the low-error rate regime where the performance targets of practical storage system are actually set. In contrast, we show that the specific structure of our concatenation coupled with the suggested decoding iteration method allows computation of the error rate upper-bound in the extremely low error rate regime, thus ensuring the satisfactory low-error-rate performance of the proposed error control scheme. Our analysis is based on estimating the probabilities of the occurrences for the particular stopping sets at the RS decoder output, which are known to fail the given outer LDPC code.

The rest of the paper is organized as follows. Section II presents the model of magnetic tape storage when viewed as a type of communication channel based on the input symbols, channel noise/disturbances and observed channel outputs. This section also provides an overview of the conventional RS-RS concatenation coding scheme in the specific LTO-5 standard. Section III gives a detailed description of the proposed error control scheme. The semi-analytic method for estimating symbol-error rate (SER) in the low SER regime is presented in Section IV. In Section V, comprehensive performance evaluations of the proposed and conventional schemes are carried out under different channels conditions. Finally, in Section VI, we conclude the present work.

II. TAPE SYSTEM

A. Error-Control System in LTO-5

In the new LTO-5 standard, the encoding operation starts by hierarchically dividing a chunk of user data called *data set*. The first level of partitioning gives rise to a number of *sub* data sets. Each sub data set is further divided into four *quarter* sub data sets. Each quarter sub data set is independently encoded into codewords of the RS-RS concatenation. Thus, the quarter sub data set is a basic data unit of the encoding operation. In Fig. 1, the quarter sub data sets are denoted by Q_i for $0 \leq i \leq 3$, respectively.

The RS-RS concatenation is also illustrated in Fig. 1 where two RS codes denoted by C_1 and C_2 are block-concatenated in the row and column directions, respectively. The outer code C_2 is a $[\tilde{n}_2, \tilde{k}_2] = [96, 84]$ code whereas the inner code C_1 is

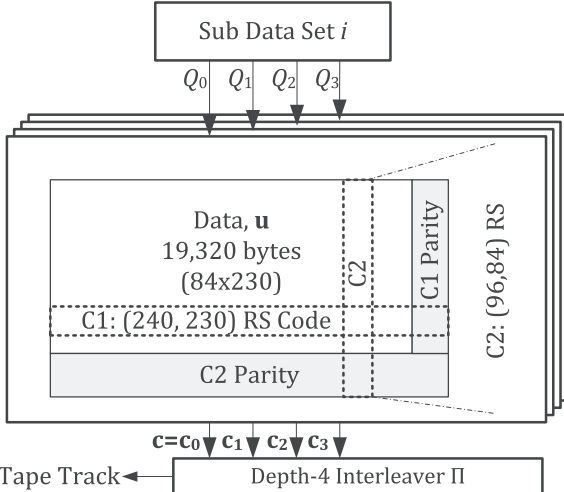


Fig. 1. The error-control system in the LTO-5 standard.

a $[\tilde{n}_1, \tilde{k}_1] = [240, 230]$ code. Both are shortened RS codes on $GF(2^8)$. More specifically, a message block of 84 bytes from a quarter sub data set is encoded into a $C2$ codeword of 96 symbols (bytes) forming a column. After 230 such columns are constructed, each row gets encoded into a $C1$ codeword of 240 symbols, eventually creating a 96 by 240 symbol array for each quarter sub data set.

As an extra level of interleaving, four $C1$ codewords taken from the same row positions of the four quarter sub data sets are interleaved symbol-wise before written onto a given physical tape track. This depth-4 interleaving forces the error bursts running over several hundred bytes to spread out to multiple quarter sub data sets.

Such four $C1$ codewords taken from the same row positions of a sub data set form a unit called a *data packet*, and there exist another deeper level of interleaving that spreads out these data packets over widely varying locations of the physical tape media [8]. This layer of interleaving is required to prevent very large error bursts due to media defects/scratches, malfunctioning header, and/or loss of synchronization from wiping out the entire sub data set.

These two layers of interleaving make the codewords in each quarter sub data set encounter independent tape channels, which enables us to conduct performance evaluations by investigating coding schemes and tape channels specific to the quarter sub data sets. In the sequel we shall focus on a single quarter sub data set. The overall code rate of the serial concatenation is simply given by $R = R_1 \times R_2 = 0.84$ where $R_1 = 230/240$ and $R_2 = 84/96$.

The inner decoder for $C1$ is effective at correcting errors due to short fades and thermal noise. However, long bursts may occasionally wipe out entire rows of the quarter sub data set, resulting in the failures of one or more $C1$ codewords. In such cases, the message part of the failed $C1$ codewords will be fed to the $C2$ outer decoder as erasures. Subsequently, the $C2$ decoder sees an erasure channel and conducts erasure decoding. Since the rows of the coded sub data set, i.e. the data packets, are widely dispersed across tape medium, the number of erasures presented in a $C2$ codeword is typically within the error

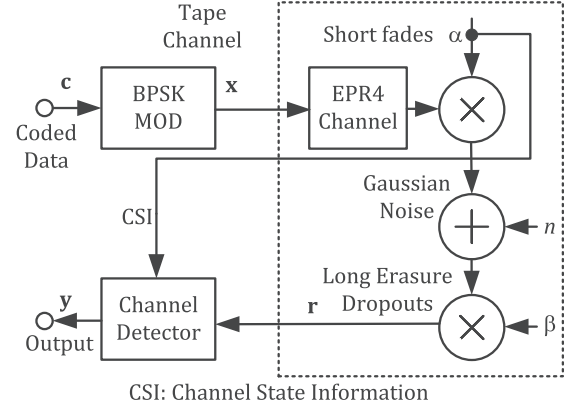


Fig. 2. An equivalent tape channel model.

correcting capability of the $C2$ code. Thus, the RS-RS concatenation with multiple levels of interleaving is designed to simultaneously correct both frequent errors of short/moderate lengths and relatively rare long error bursts. In addition, during writing the $C1$ codewords written on the tape track are immediately read and decoded to verify that no tape defects are contaminating the written data. If $C1$ decoding fails during this *read-while-write verification* stage, the failed codewords get rewritten in a different location of the tape track.

B. Channel Model

The sequence of storing and retrieving coded data in and out of the magnetic tape medium can be modeled as data transmissions over a noisy communication channel with fades and erasures. As mentioned earlier, the codeword for each quarter sub data set encounters an independent tape channel. An equivalent tape channel is shown in Fig. 2 where the non-binary codeword c gets first converted to a bipolar symbol vector x , a binary-phase-shift-keying (BPSK) representation of the codeword, which acts as the input to the tape channel. The channel itself is modeled by the extended class-4 partial response (EPR4) [31] with a system impulse response polynomial

$$h(D) = \sum_{\ell=0}^L h_\ell D^\ell = 1 + D - D^2 - D^3 \quad (1)$$

where D denotes unit delay. In addition to the usual additive white Gaussian noise (AWGN), the channel output suffers from relatively short amplitude fades and occasional long dropouts that are modeled as erasures. Specifically, the channel output observed at time i corresponding to the input x is given by

$$r_i = \beta_i \left[\alpha_i \sum_{\ell=0}^L h_\ell x_{i-\ell} + n_i \right] \quad (2)$$

where $\alpha_i \in \mathbb{R}^+$ and $\beta_i \in \{0, 1\}$ are gains corresponding to the short amplitude fade and long dropouts, respectively, x_i is the element of x , and n_i is the AWGN sample. It is assumed that the amplitude and inter-arrival time of the short fades follow exponential distributions with averages of λ_d^{-1} and λ_i^{-1} , respectively [32] and their durations (intervals over which successive

α_i 's take non-zero values) are distributed uniformly over a time range corresponding to ten to twenty RS symbols. It is also assumed that the locations of erasures and channel state information (CSI) for the short fades, i.e. β_i and α_i are known to the detector. Due to interleaving, we can assume that the long dropouts wipe out each C1 codeword independently with some probability $\Pr[\beta_i = 0] = P_\beta$ for each quarter sub data set. During the performance evaluation where we do not consider long dropouts, we simply set $P_\beta = 0$.

The channel detector, typically implemented as a Viterbi detector, releases hard decisions in the existing LTO system. But in the proposed error control system soft channel decisions will be assumed available via the Bahl-Cocke-Jelinek-Raviv (BCJR) [33] or soft-output Viterbi algorithm (SOVA) [34] equalizer. As the code employed is non-binary, soft decisions corresponding to the non-binary symbols must be generated. This can be done either by altering the channel trellis for the direct release of non-binary soft symbol decisions [35] or by converting the binary-level soft decisions to non-binary soft decisions [36].

III. THE PROPOSED ERROR-CONTROL SYSTEM

This section introduces the proposed error-control system which consists of an outer non-binary LDPC code and an inner RS code. It will be shown that despite the use of a non-binary LDPC code, this particular concatenation does not increase the overall complexity significantly while offering substantial performance advantages. An important additional merit is that the proposed concatenated code, unlike any coding scheme that utilizes an LDPC code, allows estimating error rate performance in the low error rate regime.

In the proposed RS-LDPC concatenation, the inner RS codes is the same as that of LTO-5 whereas the proposed RS-LDPC concatenation replaces the outer RS code in LTO-5 with a non-binary LDPC code over $GF(2^4)$. A pseudo-random interleaver of quarter sub data set size is assumed between the inner RS and outer LDPC codes, which allows RS coded symbols to be randomly distributed across N_{LDPC} codewords as illustrated in Fig. 3. In the encoding of the outer LDPC code, a quarter sub data set of user data are encoded into $N_{LDPC} = 23$ outer LDPC codewords of length $n_2 = 1,920$ symbols (= 960 bytes) each. Here, the field size of the non-binary LDPC code, $GF(2^4)$, is carefully selected for a reasonable compromise between complexity and performance. It should be noted that the choice of an outer LDPC code is advantageous over the conventional RS code in the sense that LDPC codes can be designed at longer codeword lengths without requiring larger finite fields, and the choice of longer LDPC codes may allow performance improvements at a linear-time growth of complexity. Note that we are not claiming that the proposed RS-LDPC concatenation is easier to implement than the existing RS-RS scheme. Our position is that the new RS-LDPC concatenation gives an opportunity to improve overall performance at the cost of increased complexity relative to the conventional RS-RS concatenation.

Since the inner and outer codes are defined over different fields in the proposed coding scheme, we treat byte symbols in and out of the outer code as groups of two consecutive four-bit symbols in an LDPC codeword as one can see in Fig. 3. That

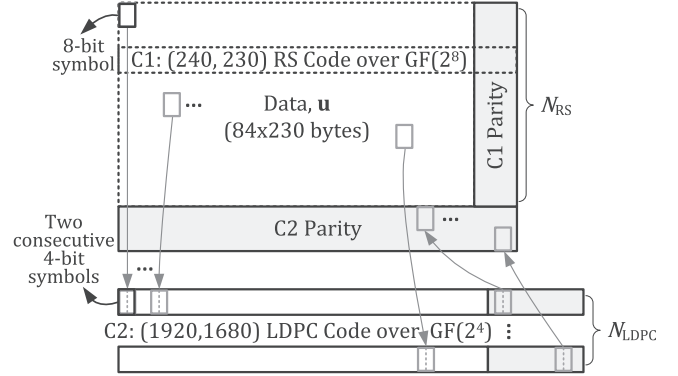


Fig. 3. A block diagram illustrating how the inner RS symbols are spread to the outer LDPC codewords through a pseudo-random interleaver.

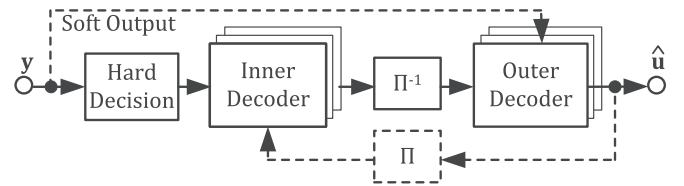


Fig. 4. Decoder block diagram for the proposed concatenated code.

is, a byte of user data amounts to two consecutive message symbols in the outer code, and blocks of two adjacent coded symbols of the outer code are fed to the inner code as message bytes. The grouping of two coded symbols is intended to minimize the number of erroneous message bytes due to a failed LDPC code. Without the grouping, a group of two four-bit symbols from a failed LDPC codeword may result in two bad message bytes of the inner RS code.

In the proposed error-control system, we assume an iterative decoding strategy shown in Fig. 4. The inner RS decoder conducts traditional hard-decision decoding. Then, the decoders for the outer LDPC codes take the hard symbol decisions from the successfully decoded RS codewords as clean symbols through the pseudo-random interleaver, as shown in Fig. 3. Meanwhile, for the failed RS codewords, the decoders for the outer LDPC codes fetch the soft outputs from the channel detector. In this work, we assume the log-domain sum-product algorithm (log-SPA) over $GF(2^4)$ [18] for decoding outer LDPC codes. In doing so, the message updating for the edges with clean symbols are simply dropped. Subsequently, the hard-decision outputs from the LDPC decoder are fed back to the RS decoder which retries decoding on the failed codewords in the earlier RS decoding. The iterations of decoding for the inner and outer codes continue in this fashion until either the LDPC decoder generates valid codewords for the entire sub data set or the number of iterations reaches a preset value. Under reasonable channel conditions, the LDPC decoder takes soft symbol decisions only occasionally; most of times its inputs will be clean hard decisions out of the inner RS decoder. This reduces the complexity of the non-binary LDPC decoder tremendously. In addition, decoding for the outer LDPC code reveals locations of clean symbols to the RS decoder, which may also simplify the Chien search and syndrome computation steps in RS decoding. The signal path denoted by the dotted lines represent data flows in the iterative decoding, while the solid lines are

in common with the single-pass decoding for the conventional coding scheme in LTO-5.

As the inner RS decoder makes clean hard decisions most of the times, the majority of the edges in the factor graph representation of the LDPC code are effectively removed. Since the complexity level of the SPA [17], [18] is directly proportional to the number of edges, the LDPC decoder complexity becomes manageable in the particular proposed concatenation structure. According to the results in [18], the average number of message additions in the variable node update for each iteration is given by

$$uM(t-1)(q-1)$$

where q is the field size of the non-binary LDPC code, M is the number of check nodes, and t and u represent the mean values of variable node and check node degrees, respectively. When the decoder failure rate of the RS inner code is given by ϕ , the effective number of edges gets reduced to $uM\phi$, and thus the number of additions turns out to be

$$uM\phi(t-1)(q-1).$$

Similarly, the numbers of additions and max* [18] operations in the check node update also reduce to

$$2(3u\phi - 4)M(q-1)^2$$

from $2(3u - 4)M(q-1)^2$. The effective number of edges is further reduced as the iteration between the decodings for the inner and outer codes continues. It should be noted that in storage applications, the operating SNR is in general higher to achieve a very low target SER than those in other applications, e.g. wireless communication. Thus, the failure rate of the inner RS code, ϕ may be much smaller, which makes the decoding for the outer LDPC code particularly efficient computationally.

It should also be noted that performance of the proposed error-control system can be further improved by introducing iterations between the channel detector and decoders. However, this extension will significantly increase latency and complexity while also rendering the performance analysis highly intractable. We will thus not consider this extension in the present work.

IV. LOWER-RATE PERFORMANCE ANALYSIS

In this section, we develop a performance evaluation technique for the proposed error-control system in the low SER regime. Again, the proposed system consists of the inner RS and outer LDPC codes, and inner/outer global iteration (IOI) is possible between the corresponding decoders. The challenge in evaluating performance of the proposed scheme lies in theoretical performance analysis of LDPC codes. Error rate evaluation for LDPC codes is largely an open problem and resort is typically made to computer simulation, which in our case is not feasible due to the extremely low target symbol (byte) error rate of 10^{-19} [6]. To resolve this technical challenge, we consider an iterative decoding strategy in Fig. 5 which is sub-optimal

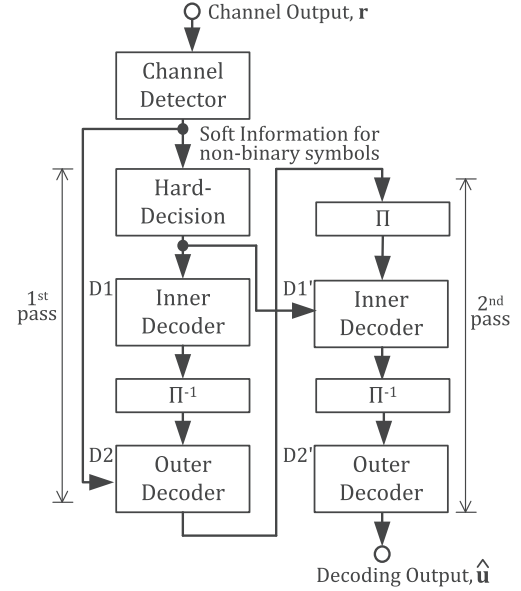


Fig. 5. Sub-optimal decoding strategy for performance analysis.

in the sense that the number of IOI is limited to two, and the decoders for the inner and outer codes do not fully utilize the information embedded in their inputs. The performance of this sub-optimal decoding system will represent an achievable performance bound of the proposed scheme. We are mainly interested in ensuring an absence of any error floors above the target SER of 10^{-19} . The sub-optimal decoding strategy is summarized as follows:

1st pass

The decodings for the inner RS and outer LDPC codes are the same as the ones introduced in Section III.

2nd pass

In the second pass, the decodings for the inner RS and outer LDPC codes are modified as follows:

- Inner RS decoding: The RS codewords are reassembled with symbols from successfully decoded LDPC codewords through the interleaver as well as the *hard-decision* outputs of the channel detector for the symbols of the failed LDPC codewords, as illustrated in Fig. 5. The inner RS decoding, $D1'$ in Fig. 5, is performed on the reassembled RS codewords.
- Outer LDPC decoding: the decoder marks the symbols in the failed RS codewords as erasures and carries out erasure decoding [37] denoted by $D2'$.

While the decoding strategy is obviously not optimal, it allows mathematically analysis that leads to a fairly tight upper bound on the SER performance. The analysis of the sub-optimal decoding strategy is carried out in such a way that we evaluate the decoding failure probability of the LDPC decoding in the first pass with computer simulation down to a reasonable SER range. We then analytically evaluate the inner RS decoding failure probability and the probability of the decoding failure event for the outer LDPC codes. In the sequel, we first do the semi-analytic performance evaluation for the memory-less AWGN channel and then for more realistic EPR4 tape channels flagged by combinations of short fades and long erasure dropouts.

A. Analysis for the AWGN Channel

Since we have the probability of the decoding failure event for the outer LDPC code from simulations, the analysis starts with the decoding for the inner RS code in the second pass. Assuming that there are N_{LDPC} LDPC codewords within a quarter sub data set, the decoding failure rate for the inner RS code in the second pass is given by

$$\Pr(\text{DF}_{\text{RS}}^{(2)}) = \sum_{i=1}^{N_{\text{LDPC}}} \Pr(F_{\text{LDPC}}^{(1)} = i) \Pr(\text{DF}_{\text{RS}}^{(2)} | F_{\text{LDPC}}^{(1)} = i) \quad (3)$$

where $F_{\text{LDPC}}^{(1)}$ is the number of failed LDPC codewords in the first pass, $\text{DF}_{\text{RS}}^{(2)}$ indicates the decoding failure event of the inner RS code in the second pass. The assumption of an AWGN channel enables us to model the probability of i failed LDPC codewords as a binomial distribution even with a simple block interleaver between the inner and outer codes. Thus, the decoding failure rate for the inner RS code can be expressed as

$$\begin{aligned} & \Pr(F_{\text{LDPC}}^{(1)} = i) \\ &= \binom{N_{\text{LDPC}}}{i} \left(\Pr(\text{DF}_{\text{LDPC}}^{(1)}) \right)^i \left(1 - \Pr(\text{DF}_{\text{LDPC}}^{(1)}) \right)^{N_{\text{LDPC}}-i} \end{aligned} \quad (4)$$

where $\binom{n}{i}$ is the binomial coefficient and $\Pr(\text{DF}_{\text{LDPC}}^{(1)})$ is the failure probability of the LDPC decoding in the first pass.

The interleaver between the inner/outer codes is designed to distribute an equal number of bad symbols across failed inner codewords as they are passed to the outer LDPC code and vice versa. Assuming that each outer LDPC codeword takes v coded symbols from an RS codeword, in the modified sub-optimal decoding strategy, the inner RS code takes v hard-decisions from the channel detector for each failed LDPC codeword, and the decoding failure probability is simply given by

$$\begin{aligned} & \Pr(\text{DF}_{\text{RS}}^{(2)} | F_{\text{LDPC}}^{(1)} = i) \\ &= \sum_{j>t_1}^{vi+m_1} \binom{vi+m_1}{j} P_{\text{raw}}^j (1 - P_{\text{raw}})^{vi+m_1-j} \end{aligned} \quad (5)$$

where $m_1 = n_1 - k_1$ and t_1 are the number of parity symbols and the error-correcting capability of the inner RS code, respectively, and P_{raw} is the raw symbol error probability at the detector output. For our specific system, we have $N_{\text{LDPC}} = 23$, $v = 10$, $m_1 = 10$, and thus $t_1 = 5$. Then, the decoding failure probability in (3) can be readily evaluated once the failure rate of the outer LDPC code, $\Pr(\text{DF}_{\text{LDPC}}^{(1)})$, is provided via simulation.

In the second pass, an erasure decoding, D2' in Fig. 5, is assumed for the outer LDPC code. The decoding failure occurs when a specific combination of failed RS codewords, equivalently a combination of erasures, forms a stopping set in the outer LDPC code. Thus, for small i values, we can carry out exhaustive search to see whether some combinations of failed RS codewords result in stopping sets in the outer LDPC code. In

general, the test should be done for $\binom{n_2}{i}$ erasure patterns which may increase fast with growing LDPC codeword length, n_2 . However, in our case, it should be noted that the test should be done for only a limited number of patterns. That is, a failed RS codeword leads to a fixed erasure pattern in each LDPC code, and the erasure pattern depends only on the structure of the interleaver. Thus, only $\binom{N_{\text{RS}}}{i}$ different combinations need to be tested to see whether each of them leads to a stopping set. Considering that $N_{\text{RS}} \ll n_2$ and N_{RS} is independent of the outer LDPC code length, the stopping set search can be done efficiently. Accordingly, the failure rate of the outer LDPC code in the second pass is given by

$$\begin{aligned} \Pr(\text{DF}_{\text{LDPC}}^{(2)}) &= \sum_{i=1}^{N_{\text{RS}}} S(i, N_{\text{RS}}) \\ &\times \Pr(\text{DF}_{\text{RS}}^{(2)})^i \left(1 - \Pr(\text{DF}_{\text{RS}}^{(2)}) \right)^{N_{\text{RS}}-i} \end{aligned} \quad (6)$$

where $S(i, N_{\text{RS}})$ is the number of combinations of i failed RS codewords resulting in stopping sets. Obviously $S(i, N_{\text{RS}}) \leq \binom{N_{\text{RS}}}{i}$. While $S(i, N_{\text{RS}})$ can be efficiently computed for small i , it may be infeasible as i increases. Thus, we instead evaluate an upper bound of (6) as

$$\begin{aligned} & \Pr(\text{DF}_{\text{LDPC}}^{(2)}) \\ &\leq \sum_{i=1}^{\gamma} S(i, N_{\text{RS}}) \Pr(\text{DF}_{\text{RS}}^{(2)})^i \left(1 - \Pr(\text{DF}_{\text{RS}}^{(2)}) \right)^{N_{\text{RS}}-i} \\ &+ \sum_{j=\gamma+1}^{N_{\text{RS}}} \binom{N_{\text{RS}}}{j} \Pr(\text{DF}_{\text{RS}}^{(2)})^j \left(1 - \Pr(\text{DF}_{\text{RS}}^{(2)}) \right)^{N_{\text{RS}}-j} \end{aligned} \quad (7)$$

where γ is chosen large enough that the evaluation of $S(\gamma, N_{\text{RS}})$ can be done within a reasonable time. The choice of γ depends on N_{RS} and the structure of the outer LDPC code as well. We will evaluate the failure rate in (7) using a specific LDPC code in Section V.

B. Analysis for the EPR4 Channel With AWGN and Short Fades

We continue our error rate analysis for the proposed RS-LDPC coding system under the assumption that the outputs from the EPR4 channel are corrupted by both short amplitude fades and Gaussian noise, as a reflection of the more realistic magnetic tape channel. Short fades are signal amplitude reductions due to reading off-azimuth data and/or variations in head-to-medium spacing. The ISI due to the EPR4 channel and the short fades make the symbol error events of inner RS codes no longer independent. This in turn induces strong correlation among the decoding failure events of the outer LDPC code, and the binomial assumption in (4) is no longer valid unless a special care is taken. The correlation makes the theoretical analysis of the proposed system more challenging. To resolve this issue, we assume a pseudo-random interleaver with dimensions matching the quarter sub data set array between the inner RS and outer LDPC codes. The pseudo-random interleaver is designed in such a way that the RS coded symbols are randomly distributed across N_{LDPC} LDPC codewords preventing

the correlated channel symbols from falling in the same LDPC codeword. The interleaver enables us to model $\Pr(F_{\text{LDPC}}^{(1)} = i)$ in (4) assuming a binomial distribution for the decoder failure probability for the individual LDPC codes, $\Pr(\text{DF}_{\text{LDPC}}^{(1)})$, in the first pass.

Now, it is necessary to find the conditional probability of (5) which is to be used in the evaluation of the failure rate of the inner RS code in (3). Recall that in our sub-optimal decoding strategy specifically designed to enable error rate analysis, we erase all bytes, i.e. groups of two consecutive symbols, in failed LDPC code words in the first decoding pass and after these bytes find their positions in the rows of the quarter sub data set through a random shuffling, we replace them with hard byte decisions from the channel detector before running the RS decoder in the second pass. Computing the RS decoder failure rate in the second pass is the prerequisite to eventually attempting the computation of the LDPC decoder failure rate in the second pass.

The RS decoder failure rate in the second pass can be computed based on the probability of i LDPC codeword failures within the quarter sub data set as well as the conditional probability of finding m bytes from failed LDPC codewords in the same positions as the bad channel bytes in a given row. This probability is needed in finding the conditional probability of seeing m erased LDPC decoder output bytes colliding with the j bad channel bytes in a given row, assuming i LDPC decoder failures.

In the derivation, though, we assume that the numbers of bad channel bytes falling into the message and parity regions (resp. j and ℓ) are statistically independent, i.e., $\Pr[j, \ell] = \Pr[j]\Pr[\ell]$, an assumption necessary to make the overall analysis mathematically tractable. Since the average burst length due to the short fades is relatively short compared to the length of the C1 code, the depth-4 interleaver at the channel input mentioned earlier allow us to assume that the statistics on the numbers of bad channel bytes in the message region versus the parity region are independent of each other. In Section V, we will verify empirically that $\Pr[j|\ell]$, the conditional probability of seeing j bad channel bytes falling in the message region given that ℓ bad channel bytes fell in the parity region, is indeed not a function of ℓ . With this assumption, we can express the failure rate of the inner RS code as

$$\begin{aligned} \Pr\left(\text{DF}_{\text{RS}}^{(2)} \mid F_{\text{LDPC}}^{(1)} = i\right) &= \sum_{\ell=0}^{m_1} \sum_{j=j^*}^{k_1} \sum_{m=m^*}^j \Pr[m, j, \ell|i] \\ &= \sum_{\ell=0}^{m_1} \sum_{j=j^*}^{k_1} \sum_{m=m^*}^j \Pr[m|j, \ell, i] \Pr[j, \ell|i] \quad (8) \\ &= \sum_{\ell=0}^{m_1} \sum_{j=j^*}^{k_1} \sum_{m=m^*}^j \Pr[m|j, i] \Pr[j] \Pr[\ell] \quad (9) \end{aligned}$$

where $j^* = m^* = \max(t_1 + 1 - \ell, 1)$,

$$\Pr[m|j, i] = \binom{j}{m} \left(\frac{i}{N_{\text{LDPC}}}\right)^m \left(1 - \frac{i}{N_{\text{LDPC}}}\right)^{j-m} \quad (10)$$

and $\Pr[j]$ and $\Pr[\ell]$ are empirical distributions, and $\max(t_1 + 1 - \ell, 1)$ gives the maximum number of bad bytes in the message region in a failed RS codeword given ℓ bad bytes in the parity region. The equalities in (8) and (9) hold due to the chain rule of conditional probability and the fact that the number bad bytes colliding with erased LDPC coded symbols is independent of the number of bad bytes in the parity region, respectively. Since a random interleaver and i failed LDPC codes are assumed, the probability for an RS coded symbol to be taken from a failed LDPC code is given by i/N_{LDPC} , which directly leads to the conditional probability in (10).

Now, an upper bound on the LDPC failure rate in (7) can be readily computed by enumerating the number of stopping sets, i.e. $S(i, N_{\text{RS}})$. In contrast to the block interleaver in the AWGN case, the random interleaver results in different erasure patterns fed to N_{LDPC} LDPC codes. Accordingly, the maximum number of stopping sets should be increased to $N_{\text{LDPC}} \cdot \binom{N_{\text{RS}}}{i}$, i.e., $S(i, N_{\text{RS}}) \leq N_{\text{LDPC}} \cdot \binom{N_{\text{RS}}}{i}$. In Section V, the numbers of stopping sets are enumerated at $i = 1, 2, \dots, 5$ for the designed pseudo-random interleaver.

C. Analysis for the Channel With Long Dropouts

Performance evaluation of the proposed system is also carried out on a channel that is also flagged by long dropouts in addition to ISI and AWGN. It is assumed that the long dropouts arose from erasure of read signals along an entire track out of N_t tracks, which usually happens due to a synchronization loss. In LTO-5, $N_t = 16$ tracks are employed.

To cope with the long dropouts, in LTO-5, C1 codewords in the same row from a sub data set are assembled into a data packet. The data packets in a data set are widely interleaved in such a way that they are uniformly scattered across N_t tracks. Thus, the one track loss leads to erasures of $N_e (= N_{\text{RS}}/N_t)$ C1 codewords in every quarter sub data set. If an LDPC code fails in the first pass of IOI, all the N_e erased RS codewords have at least one byte from the failed LDPC code. Thus, none of the erased RS codewords can be recovered in the second pass of IOI. Meanwhile, the failure rate of the remaining $N_{\text{RS}} - N_e$ RS codewords is the same as that in (9).

Finally, to get the failure rate of LDPC codes after the second pass, the enumeration for the stopping sets must be conducted. In doing so, erasure patterns from N_t different track losses should be considered in addition to failed RS codes among the remaining $(N_{\text{RS}} - N_e)$ RS codes. Thus, when there are i failed RS codes out of the $(N_{\text{RS}} - N_e)$ RS codes, the maximum number of distinct erasure patterns becomes $\binom{N_{\text{RS}} - N_e}{i} \cdot (N_{\text{LDPC}} N_t)$, and the failure rate of the LDPC codes in the second pass can be expressed as

$$\begin{aligned} \Pr\left(\text{DF}_{\text{LDPC}}^{(2)}\right) &= \sum_{i=1}^{N_{\text{RS}} - N_e} S(i, N_{\text{RS}}) \\ &\times \Pr\left(\text{DF}_{\text{RS}}^{(2)}\right)^i \left(1 - \Pr\left(\text{DF}_{\text{RS}}^{(2)}\right)\right)^{(N_{\text{RS}} - N_e) - i} \end{aligned} \quad (11)$$

where $S(i, N_{\text{RS}}) \leq \binom{N_{\text{RS}} - N_e}{i} \cdot (N_{\text{LDPC}} N_t)$. In Section V, the numbers of stopping sets are enumerated at $i = 1, 2$.

V. PERFORMANCE COMPARISONS

In this section, we first evaluate performances of the systems with the proposed RS-LDPC and conventional RS-RS concatenations on various channels representing magnetic tape systems using simulations down to the SER range of $10^{-5} - 10^{-6}$. The performance evaluations for the two systems clearly show that the proposed system outperforms the conventional one by a large margin. We then show that the extrapolations of the simulated SER curves of the proposed scheme to low SER region are valid based on the results of the bounds derived in the last section. It will be shown that the evaluated bounds indeed preclude the presence of error floors well below the target SER of the practical tape system.

For the performance evaluations, we employ a specific non-binary LDPC code over $\text{GF}(2^4)$ of a rate 0.875 as the outer code, which has a regular structure with the degree distribution pair given by $\lambda(x) = x^3$ and $\rho(x) = x^{24}$. In order to construct this non-binary LDPC code, we first designed a binary parity-check matrix for codewords of length $n_2 = 1,920$ using the progressive edge growth (PEG) algorithm [22]. The non-zero entries in the resulting binary parity-check matrix are then replaced with randomly selected elements in $\text{GF}(2^4)$ except for zeros [38].¹ The log-SPA [18] is used for decoding the so constructed ($n_2 = 1920, k_2 = 1680$) LDPC code over $\text{GF}(2^4)$ with a maximum of 50 iterations. The log-SPA decoding for non-binary LDPC codes can be greatly accelerated by taking advantage of the RS decoding results as discussed in Section III. Since the proposed system assumes iterations between the inner and outer decoders, for the comparisons to be fair, we also assume that an iterative decoding strategy is employed for the conventional coding scheme. In particular, in the iterative decoding strategy, hard-decision decoding is performed for the inner/outer RS codes except for the last iteration in which an erasure decoding is done for the outer RS code. The inner/outer iteration is halted after a maximum of five IOIs, which is the same as in the proposed decoding strategy.

SER simulations are first done on the AWGN channels with/without long dropouts. We conduct simulations on the AWGN channel without long dropouts in Fig. 6 where it is observed that the proposed system outperforms the conventional one by 1.6 dB at a SER of 10^{-5} . This coding gain comes mainly from the fact that the proposed scheme takes advantage of the soft information from the channel detector. In Fig. 7, the performance of the proposed scheme is also shown for different numbers of IOIs. The results in Fig. 7 show that the SER improves with each additional iteration, but with a quickly diminishing gain. We shall simply set the maximum number of IOIs to five for the subsequent performance evaluations. To see the effect of long dropouts, the channel with AWGN and long dropouts is considered in such a way that 7 out of 96 rows in a quarter sub data set are completely erased, which implies a complete dead track with additional 32 data packets erased within a data set. When long dropouts are present, the channel behaves more like an erasure channel, and the performance superiority of the proposed scheme over the conventional RS-RS concatenation diminishes since RS codes are optimal on

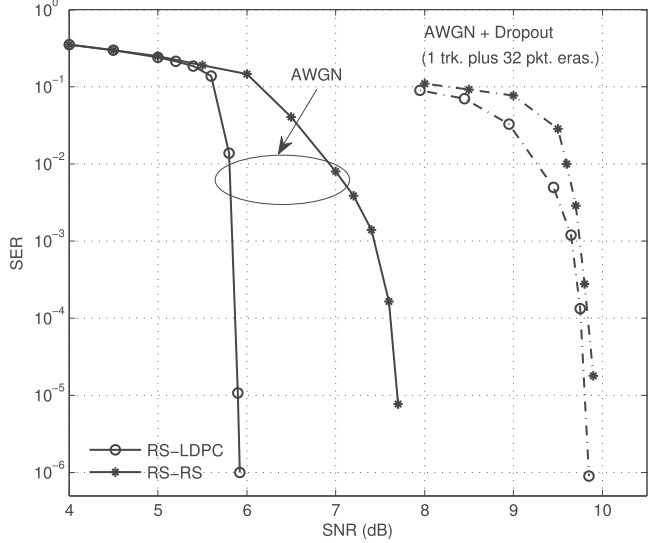


Fig. 6. SER performance evaluations of the proposed and conventional schemes over AWGN channel with/without long dropouts.

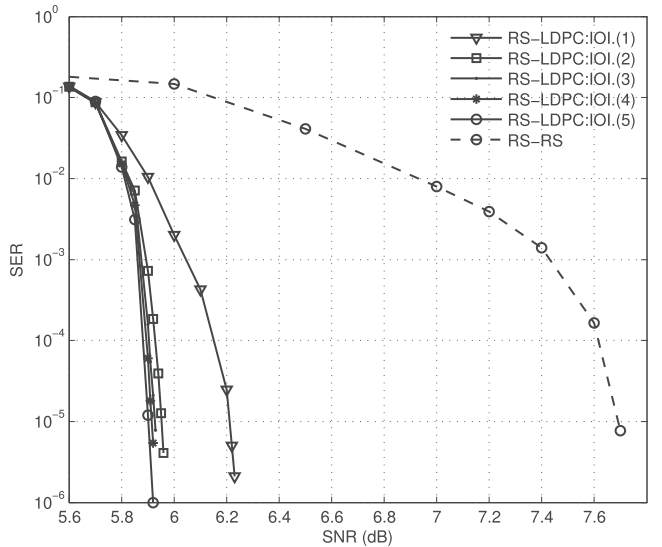


Fig. 7. SER performance evaluations of the proposed schemes with different numbers of IOIs over AWGN channel.

erasure channels. Nevertheless, the proposed scheme shows a comparable performance to that of the RS coding scheme on the erasure channel.

Next, we carry out performance evaluations on a more realistic channel, i.e., a combination of EPR4, short fades and AWGN. That is, the output symbols from the EPR4 channel are corrupted by both short amplitude fades and Gaussian noise. In the modeling of short fades, we assume that the fade duration is uniformly distributed in the range 10-20 bytes while both the amplitude and the inter-arrival distance follow independent exponential distributions with $\lambda_d^{-1} = 0.2$ and $\lambda_i^{-1} = 800$ bytes, respectively. The performance comparisons in Fig. 8 show that the proposed scheme outperforms the conventional one by about 1.45 dB at a SER of 10^{-5} .

Finally, we carry out the performance comparisons on the EPR4 channel with long dropouts instead of the short fades.

¹The parity-check matrix is available online [39].

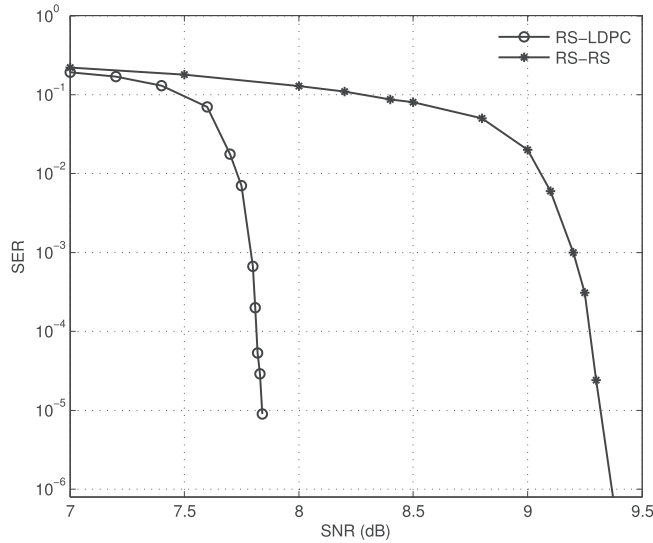


Fig. 8. SER performance evaluations of the proposed and conventional schemes over a channel with EPR4, short fades and AWGN.

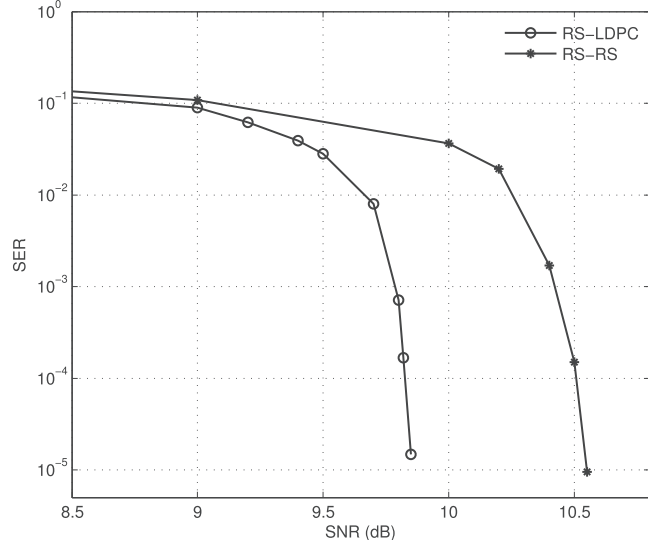


Fig. 9. SER performance evaluations of the proposed and conventional schemes over a channel with EPR4, AWGN and long dropout.

The long dropout represents a complete dead track which erases $N_e = 6$ out of $N_{RS} = 96$ rows in a quarter sub data set. The results are depicted in Fig. 9 where the proposed scheme has about 0.7 dB gain over the conventional scheme. As observed in the AWGN case, the performance gain is somewhat reduced when long dropouts are present.

Now, using the analysis technique developed in Section IV, we will evaluate the performance-bounds of the proposed system in the low SER regime on the channels considered in the performance evaluations. Since the analysis technique provides an upper bound on the decoder failure rate, the results can be taken as guaranteed worst-case performances at SNRs of interest. The evaluation for the upper bound in (7) is carried out in such a way that we first find $\Pr(\text{DF}_{RS}^{(2)})$ in (3) which is related to the raw SER (denoted by P_{raw}) and $\Pr(\text{DF}_{LDPC}^{(1)})$ through the relations in (4) and (5). Later, the stopping sets $S(i, N_{RS})$

TABLE I
 $S(i, N_{RS})$ FOR AWGN AND EPR4 + FADE CHANNELS WHEN $\gamma = 5$; X STANDS FOR $\binom{N_{RS}-N_e}{i} \cdot (N_{LDPC} N_t)$

i	1	2	3	4	5
AWGN	0	0	0	5	468
EPR4 + short fades	0	0	11	1134	57677
EPR4 + long dropouts	0	38520	X	X	X

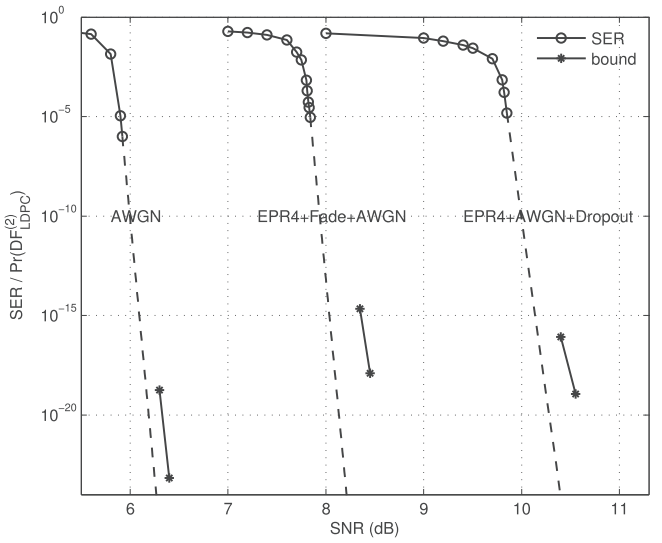


Fig. 10. Extrapolations of simulated SER curves and bounds on memoryless AWGN channel and EPR4 channels with AWGN with short fades/long dropouts.

for $1 \leq i \leq \gamma$ are enumerated up to the case with γ failed RS codes.

The evaluation is performed at a SNR of 6.4 dB where P_{raw} and $\Pr(\text{DF}_{LDPC}^{(1)})$ are found to be 1.38×10^{-1} and 10^{-6} , respectively. The LDPC failure rate in the first pass of IOI, $\Pr(\text{DF}_{LDPC}^{(1)})$, is obtained from the simulation results. The search for stopping sets is conducted up to five failed RS codes, i.e. $\gamma = 5$. In the search, it is found that no stopping sets arise until the number of failed RS codewords reaches beyond three, i.e. $S(i, N_{RS}) = 0$ for $i = 1, 2, 3$. For four and five failed RS codes, there are $\binom{96}{4}$ and $\binom{96}{5}$ possibilities, respectively, among which only $S(4, N_{RS}) = 5$ and $S(5, N_{RS}) = 468$ cases give rise to stopping sets in the LDPC decoding. The results are summarized in the first row of Table I. By taking the results for $S(i, N_{RS})$ and $\Pr(\text{DF}_{RS}^{(2)})$ to the upper bound in (7), we arrive at an achievable bound of 6.94×10^{-24} at SNR of 6.4 dB. On the other hand, at the same operating SNR of 6.4 dB, the SER of the conventional system is at around 10^{-2} , which clearly shows that the proposed system provides unparalleled performance improvements over the conventional one on the AWGN channel. The upper bound is re-evaluated at a lower SNR value of 6.3 dB, and the bounds are compared with the extrapolated simulation results in Fig. 10.

For the EPR4 channel with a combination of short fades and AWGN, we evaluate the bound of (11). Following the similar steps, we first evaluate $\Pr(\text{DF}_{RS}^{(2)})$ by utilizing (9) and enumerating stopping sets $S(i, N_{RS})$ for $1 \leq i \leq \gamma$. As mentioned earlier, however, the derivation in (9) relies on the assumption

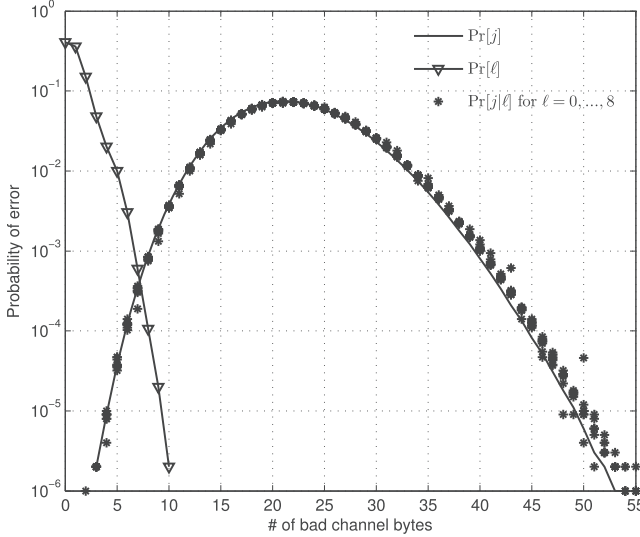


Fig. 11. Empirical distributions of $\Pr[j]$, $\Pr[\ell]$ and $\Pr[j|\ell]$ for $\ell = 0, 1, \dots, 8$ over the EPR4 channel with short fades and AWGN at a SNR of 8.45dB.

that the numbers of bad bytes falling in message versus parity regions, j and ℓ , respectively, are statistically independent, and thus the joint distribution can be expressed as a product of marginal distributions, $\Pr[j, \ell] = \Pr[j]\Pr[\ell]$. To confirm this assumption, the distributions $\Pr[j|\ell]$ obtained empirically are plotted while varying ℓ from 0 to 8 in Fig. 11. It is seen that regardless of the value of ℓ , the samples of $\Pr[j|\ell]$ all contribute to outlining a single curve, which is labeled as $\Pr[\ell]$, confirming that $\Pr[j|\ell]$ does not depend on ℓ . The empirical distributions have been gathered assuming that the duration of short amplitude fades results in an average burst length of 2-5 bytes in C1 due to the interleaver structure at the channel input. The data is collected at an SNR of 8.45 dB. Fig. 11 also shows empirical distributions of $\Pr[j]$ and $\Pr[\ell]$.

Meanwhile, the LDPC failure rate $\Pr(\text{DF}_{\text{LDPC}}^{(1)}) = 10^{-6}$ at the same SNR of 8.45 dB is observed for the channel considered for generating the curves in Fig. 8. The corresponding RS code failure rate in the second pass, $\Pr(\text{DF}_{\text{RS}}^{(2)})$, can be computed by taking the empirical result into (9), which leads to $\Pr(\text{DF}_{\text{RS}}^{(2)}) = 4.84 \times 10^{-7}$. Finally, the evaluation of the upper bound in (11) with $S(i, N_{\text{LDPC}})$ in the second row of Table I indicates that the upper bound on the LDPC failure rate in the second pass, $\Pr(\text{DF}_2^{(2)})$, is 1.24×10^{-18} , which is more than satisfactory. The evaluation of the upper bound is repeated at a SNR of 8.35 dB, and the result is shown along with the extrapolated simulation results in Fig. 10.

Finally, the decoder failure rate $\Pr(\text{DF}_{\text{LDPC}}^{(2)})$ for the EPR4 channel with AWGN and long erasure dropouts is evaluated. In doing so, as the first step, $\Pr(\text{DF}_{\text{LDPC}}^{(1)})$ is taken from the simulation results where $\Pr(\text{DF}_{\text{LDPC}}^{(1)}) = 10^{-6}$ is seen to be achieved at SNR of 10.55 dB. Then, the RS code failure rate in the second pass, $\Pr(\text{DF}_{\text{RS}}^{(2)})$ in (9), becomes 1.7×10^{-12} , which in turn results in a LDPC code failure rate in the second pass, $\Pr(\text{DF}_{\text{LDPC}}^{(2)})$, of 1.12×10^{-19} . It should be noted that stopping sets listed in the third row of Table I are caused by $N_e + i$ erased RS codes, and the number of combinations of failed RS codes

grows fast with increasing i . Thus, the search for the stopping sets is conducted only up to $\gamma = 2$. Still, it can be seen that the bound is reasonably tight. The evaluation for the upper bound on $\Pr(\text{DF}_{\text{LDPC}}^{(2)})$ is conducted again at a SNR of 10.4 dB, and the bounds are compared with the extrapolation of the simulations results in Fig. 10. The evaluated bounds confirm that there are no error floors for the proposed RS-LDPC concatenated coding system down to the target SER range around 10^{-19} .

VI. CONCLUSIONS

We proposed a novel error-control system utilizing RS-LDPC concatenation for the modern tape channel plagued by different types of error mechanisms. The proposed scheme is significant in that 1) it gives large performance gain with respect to the conventional RS-RS concatenation while performing comparable to the latter in erasure-dominant channels, 2) despite the use of a non-binary LDPC outer code, the utilization of hard RS decoder decisions most of the time makes the decoding complexity quite manageable, and 3) unlike any coding scheme relying on LDPC codes, the proposed scheme allows performance analysis in low-error-rate regime. The theoretical bound analysis indeed has confirmed that the proposed coding scheme does not suffer from the usual error floor issues of LDPC codes. While the current paper focuses on the tape channel, the particular proposed concatenation finds applications in other important areas including wireless channels with block fading and power-line channels.

ACKNOWLEDGMENT

The authors are indebted by the encouragements, feedback and constructive criticisms provided by Drs. Thomas Mittelholzer and Roy Cideciyan of IBM Research and Drs. JW Lee and Suayb Arslan of Quantum Corporation throughout the project.

REFERENCES

- [1] R. H. Dee, "Magnetic tape for data storage: An enduring technology," *Proc. IEEE*, vol. 96, no. 11, pp. 1775–1785, Nov. 2008.
- [2] E. Childers, W. Imai, J. Eaton, G. Jaquette, P. Koeppe, and D. Hellman, "Six orders of magnitude in linear tape technology: The one-terabyte project," *IBM J. Res. Develop.*, vol. 47, no. 4, pp. 471–482, Jul. 2003.
- [3] R. H. Dee, "The challenges of magnetic recording on tape for data storage (the one terabyte cartridge and beyond)," in *Proc. 10th NASA Goddard Space Flight Center Conf. Mass Storage Syst. Technol.*, Apr. 2002, pp. 109–119.
- [4] R. H. Dee, "Magnetic tape: The challenge of reaching hard-disk-drive data densities on flexible media," *MRS Bull.*, vol. 31, pp. 404–408, May 2006.
- [5] Information Storage Industry Consortium (INSIC). (2005). *Magnetic Tape Storage Roadmap*, San Diego, CA, USA [Online]. Available: <http://www.insic.org>
- [6] Information Storage Industry Consortium (INSIC). (2012, Mar.). *International Magnetic Tape Storage Roadmap* [Online]. Available: <http://www.insic.org>
- [7] S. Sankaranarayanan and E. Eleftheriou, "Performance of product codes on channels with memory," in *Proc. IEEE Int. Symp. Inf. Theory*, Sep. 2005, pp. 548–552.
- [8] *Data Interchange on 12.7 mm 384-Track Magnetic Tape Cartridges*, ECMA-319 Standard, 2001.
- [9] S. Sahu, H. Song, and B. Vijaya Kumar, "Performance of low-density parity-check (LDPC) codes on high-density magnetic tape recording signals," in *Proc. IEEE Int. Magn. Conf.*, Mar. 2003, pp. DT-10.

- [10] Y. Han and W. Ryan, "Packet-LDPC codes for tape drives," *IEEE Trans. Magn.*, vol. 41, no. 4, pp. 1340–1347, Apr. 2005.
- [11] Y. Han, W. Ryan, and R. Wesel, "Dual-mode decoding of product codes with application to tape storage," in *Proc. IEEE Global Telecommun. Conf.*, Nov. 2005, vol. 3, pp. 1255–1260.
- [12] Y. Han and W. Ryan, "Concatenating a structured LDPC code and a constrained code to preserve soft-decoding, structure, and burst correction," *IEEE Trans. Magn.*, vol. 42, no. 10, pp. 2558–2560, Oct. 2006.
- [13] Z. Li, J. Xie, and B. Kumar, "Low-density parity-check codes with variable rate and randomized constraints for advanced magnetic tape recording," in *Proc. IEEE Int. Magn. Conf. Asia*, Apr. 2005, pp. 1611–1612.
- [14] D. Yang, R. Molstad, and Y. Yip, "Performance evaluation of LDPC code on VR2 channel," in *Proc. IEEE Int. Magn. Conf. Eur.*, Apr. 2002, pp. AP2.
- [15] B. Liu, Y. Li, B. Rong, L. Gui, and Y. Wu, "LDPC-RS product codes for digital terrestrial broadcasting transmission system," *IEEE Trans. Broadcast.*, vol. 60, no. 1, pp. 38–49, Mar. 2014.
- [16] S. I. Park *et al.*, "LDPC-RS two dimensional code for the next generation cloud transmission system," in *Proc. IEEE Int. Symp. Broadband Multimedia Syst. Broadcast.*, Jun. 2014, pp. 1–2.
- [17] M. Davey and D. J. C MacKay, "Low density parity check codes over GF(q)," in *Proc. Inf. Theory Workshop*, 1998, pp. 70–71.
- [18] H. Wygaersch, H. Steendam, and M. Moeneclaey, "Log-domain decoding of LDPC codes over GF(q)," in *Proc. IEEE Int. Conf. Commun.*, 2004, vol. 2, pp. 772–776.
- [19] N. Andreadou and F.-N. Pavlidou, "Mitigation of impulsive noise effect on the PLC channel with QC-LDPC codes as the outer coding scheme," *IEEE Trans. Power Del.*, vol. 25, no. 3, pp. 1440–1449, Jul. 2010.
- [20] T. Richardson, "Error floors of LDPC codes," in *Proc. 41st Allerton Conf. Commun. Control Comput.*, Oct. 2003, pp. 1426–1435.
- [21] Y. Kou, S. Lin, and M. Fossorier, "Low-density parity-check codes based on finite geometries: A rediscovery and new results," *IEEE Trans. Inf. Theory*, vol. 47, no. 7, pp. 2711–2736, Nov. 2001.
- [22] X.-Y. Hu, E. Eleftheriou, and D.-M. Arnold, "Progressive edge-growth Tanner graphs," in *Proc. IEEE Global Telecommun. Conf.*, Nov. 2001, vol. 2, pp. 995–1001.
- [23] T. Tian, C. Jones, J. Villasenor, and R. Wesel, "Construction of irregular LDPC codes with low error floors," in *Proc. IEEE Int. Conf. Commun.*, May 2003, vol. 5, pp. 3125–3129.
- [24] A. Abbasfar, D. Divsalar, and K. Yao, "Accumulate-repeat-accumulate codes," *IEEE Trans. Commun.*, vol. 55, no. 4, pp. 692–702, Apr. 2007.
- [25] Y. Zhang and W. Ryan, "Structured IRA codes: Performance analysis and construction," *IEEE Trans. Commun.*, vol. 55, no. 5, pp. 837–844, May 2007.
- [26] Y. Zhang and W. Ryan, "Toward low LDPC-code floors: A case study," *IEEE Trans. Commun.*, vol. 57, no. 6, pp. 1566–1573, Jun. 2009.
- [27] J. Lu and J. Moura, "Structured LDPC codes for high-density recording: Large girth and low error floor," *IEEE Trans. Magn.*, vol. 42, no. 2, pp. 208–213, Feb. 2006.
- [28] H. Xiao and A. Banishashemi, "Graph-based message-passing schedules for decoding LDPC codes," *IEEE Trans. Commun.*, vol. 52, no. 12, pp. 2098–2105, Dec. 2004.
- [29] G. Liva, W. Ryan, and M. Chiani, "Quasi-cyclic generalized LDPC codes with low error floors," *IEEE Trans. Commun.*, vol. 56, no. 1, pp. 49–57, Jan. 2008.
- [30] Y. Han and W. Ryan, "Low-floor decoders for LDPC codes," *IEEE Trans. Commun.*, vol. 57, no. 6, pp. 1663–1673, Jun. 2009.
- [31] H. Thapar and A. Patel, "A class of partial response systems for increasing storage density in magnetic recording," *IEEE Trans. Magn.*, vol. 23, no. 5, pp. 3666–3668, Sep. 1987.
- [32] B. Steingrimsson and J. Moon, "Dropout compensation in magnetic tape channels by adaptive equalization and coding," *IEEE Trans. Magn.*, vol. 37, no. 6, pp. 3981–3993, Nov. 2001.
- [33] L. Bahl, J. Cocke, F. Jelinek, and J. Raviv, "Optimal decoding of linear codes for minimizing symbol error rate (corresp.)," *IEEE Trans. Inf. Theory*, vol. 20, no. 2, pp. 284–287, Mar. 1974.
- [34] J. Hagenauer and P. Hoeher, "A Viterbi algorithm with soft-decision outputs and its applications," in *Proc. IEEE Global Telecommun. Conf.*, Nov. 1989, vol. 3, pp. 1680–1686.
- [35] A. Lafourcade and A. Vardy, "Optimal sectionalization of a trellis," *IEEE Trans. Inf. Theory*, vol. 42, no. 3, pp. 689–703, May 1996.
- [36] P. Hoeher, "Optimal subblock-by-subblock detection," *IEEE Trans. Commun.*, vol. 43, nos. 2–4, pp. 714–717, Feb. 1995.
- [37] V. Savin, "Non binary LDPC codes over the binary erasure channel: Density evolution analysis," in *Proc. IEEE Int. Symp. Appl. Sci. Biomed. Commun. Technol.*, Oct. 2008, pp. 1–5.

- [38] I. Djordjevic and B. Vasic, "Nonbinary LDPC codes for optical communication systems," *IEEE Photonics Technol. Lett.*, vol. 17, no. 10, pp. 2224–2226, Oct. 2005.
- [39] [Online]. Available: <https://www.dropbox.com/sh/y1xe01hew3n9vkl/AAD2AwOKaokvvLwjDlx2thea?dl=0>



Jieun Oh received the B.S. degree in electrical engineering from Handong University, Pohang, South Korea, and the M.S. and Ph.D. degrees in electrical engineering from the Korea Advanced Institute of Science and Technology (KAIST), Daejeon, South Korea, in 2009, 2011, and 2015, respectively. Her research interests include coding and information theory for the storage channels.



Jeongseok Ha (M'06) received the B.E. degree in electronics from Kyungpook National University, Daegu, South Korea, the M.S. degree in electronic and electrical engineering from Pohang University of Science and Technology, Pohang, South Korea, and the Ph.D. degree in electrical and computer engineering from the Georgia Institute of Technology, Atlanta, GA, USA, in 1992, 1994, and 2003, respectively. He is currently with the Korea Advanced Institute of Science and Technology (KAIST), Daejeon, South Korea, as an Associate Professor. His research interests include theories and applications of error-control codes and physical layer security.



Hyegyeong Park (S'12) received the B.S. and M.S. degrees in electrical engineering from the Korea Advanced Institute of Science and Technology (KAIST), Daejeon, South Korea, in 2012 and 2014, respectively. She is currently pursuing the Ph.D. degree at KAIST. Her research interests include coding and information theory with the current focus on distributed storage.



Jaekyun Moon (F'05) received the Ph.D. degree in electrical and computer engineering from Carnegie Mellon University, Pittsburgh, PA, USA. He is a Professor of Electrical Engineering with Korea Advanced Institute of Science and Technology (KAIST), Daejeon, South Korea. From 1990 to 2009, he was with the Faculty of the Department of Electrical and Computer Engineering, University of Minnesota, Twin Cities, Minneapolis, MN, USA. His research interests include channel characterization, signal processing, and coding for data storage

and digital communication. He served as the Program Chair for the 1997 IEEE Magnetic Recording Conference. He is also the Past Chair of the Signal Processing for Storage Technical Committee of the IEEE Communications Society. He served as a Guest Editor for the 2001 IEEE JOURNAL ON SELECTED AREAS IN COMMUNICATIONS issue on Signal Processing for High Density Recording. He also served as an Editor for IEEE TRANSACTIONS ON MAGNETICS in the area of signal processing and coding from 2001 to 2006. He consulted as the Chief Scientist for DSPG, Inc. from 2004 to 2007. He also worked as the Chief Technology Officer at Link-A-Media Devices Corp. He was the recipient of the McKnight Land-Grant Professorship from the University of Minnesota, and the IBM Faculty Development Awards as well as the IBM Partnership Awards. He was also the recipient of the National Storage Industry Consortium (NSIC) Technical Achievement Award for the invention of the maximum transition run (MTR) code, a widely used error-control/modulation code in commercial storage systems.